Dissociation of energy-selected c - C 2 H 4 S + in a region 10.6–11.8 eV: Threshold photoelectron—photoion coincidence experiments and quantum-chemical calculations

Yung-Sheng Fang, I-Feng Lin, Yao-Chang Lee, and Su-Yu Chiang

Citation: The Journal of Chemical Physics **123**, 054312 (2005); doi: 10.1063/1.1993589
View online: http://dx.doi.org/10.1063/1.1993589
View Table of Contents: http://scitation.aip.org/content/aip/journal/jcp/123/5?ver=pdfcov
Published by the AIP Publishing

Dissociation of energy-selected c-$C_2H_4S^+$ in a region 10.6–11.8 eV: Threshold photoelectron—photoion coincidence experiments and quantum-chemical calculations

Yung-Sheng Fang
Department of Applied Chemistry, National Chiao Tung University, 1001, Ta Hsueh Road, Hsinchu 30010, Taiwan

I-Feng Lin, Yao-Chang Lee, and Su-Yu Chiang[a)]
National Synchrotron Radiation Research Center, 101, Hsin Ann Road, Hsinchu Science Park, Hsinchu 30076, Taiwan

(Received 20 January 2005; accepted 13 June 2005; published online 9 August 2005)

Dissociation of energy-selected c-$C_2H_4S^+$ was investigated in a region of 10.6–11.8 eV with a threshold photoelectron-photoion coincidence technique and a synchrotron as a source of vacuum ultraviolet radiation. Branching ratios and average releases of kinetic energy in channels of formation of c-$C_2H_4S^+$, CH_3CS^+, and HCS^+ were obtained from well-resolved time-of-flight peaks in coincidence mass spectra. Measured average releases of kinetic energy for channel $CH_3CS^+ + H$ of least energy are substantial and much greater than calculated with quasiequilibrium theory; in contrast, small releases of kinetic energy near the appearance onset for channel $HCS^+ + CH_3$ agree satisfactorily with statistical calculations. Calculations of molecular electronic structures and energetics of c-$C_2H_4S^+$ and $C_2H_3S^+$ isomers and various fragments and transition states were also performed with Gaussian 3 method to establish dissociation mechanisms. A predicted dissociation energy of 11.05 eV for c-$C_2H_4S \rightarrow HCS^+ + CH_3$ agrees with a linearly extrapolated threshold at 10.99 ± 0.04 eV and a predicted dissociation mechanism that c-$C_2H_4S^+$ isomerizes to CH_3CHS^+ before dissociating to $HCS^+ + CH_3$ supports the experimental results. The large releases of kinetic energy for channel $CH_3CS^+ + H$ might result from a dissociation mechanism according to which c-$C_2H_4S^+$ isomerizes to a local minimum CH_3CSH^+ and then dissociates through a transition state to form $CH_3CS^+ + H$. © *2005 American Institute of Physics*. [DOI: 10.1063/1.1993589]

I. INTRODUCTION

Photodissociation (PD) and photoionization (PI) of thirane (c-C_2H_4S) are important topics from both experimental and theoretical perspectives because the large ring strain facilitates the ring-opening processes and isomerization, and also because they offer a powerful means of obtaining information about the structures and energetics of important radicals and ions.[1–8] For example, photodissociation of c-C_2H_4S to form $C_2H_4 + S$ has been investigated with excitation at 193 nm;[3,9–11] understanding of energetics of triplet $C_2H_4(^3B_{1u})$ was thus obtained with photofragment-translational spectroscopy (PTS) using a tunable synchrotron light to probe products selectively.[3] Photodissociation to produce important species H_2S, C_2H_2, CH_4, H_2, and S pertinent to combustion and atmospheric chemistry was also reported with excitation in the region of 180–240 nm.[12]

Butler and Baer investigated the dissociative photoionization of c-C_2H_4S to form fragment ions HCS^+ and $C_2H_3S^+$ with photoionization mass spectroscopy (PIMS) and derived their heat of formation according to the determined appearance energies (AEs) and existing thermochemical data, but the derived heat of formation 245 ± 2 kcal mol^{-1} for HCS^+ is greater than 233 ± 2 kcal mol^{-1} obtained from dissociative photoionization of c-C_3H_6S and c-C_4H_8S.[1] They also determined an average release of 0.03 eV of kinetic energy for the formation of HCS^+ at the dissociation threshold from time-of-flight (TOF) peaks in photoelectron-photoion coincidence (PEPICO) spectra of c-C_2H_4S and proposed an angular structure of HCS^+ on a basis that the experimental value is significantly less than the statistically expected 0.1 eV.[1,2]

We have measured photoionization mass spectra of c-C_2H_4S in a region of ~9–20 eV using synchrotron radiation as an ionization source.[13] The experimental ionization energy (IE) at 90.51 ± 0.003 eV agrees satisfactorily with a theoretical prediction of 9.07 eV for the formation of c-$C_2H_4S^+$, reflecting a small structural alternation upon ionization. Five major fragment ions—$C_2H_3S^+$, $C_2H_2S^+$, HCS^+, H_2S^+, and $C_2H_3^+$—were observed with their respective AEs determined from the onset of photoionization efficiency (PIE) curves and six dissociation channels—c-$C_2H_4S^+ \rightarrow CH_3CS^+ + H$, $HCS^+ + CH_3$, $H_2S^+ + C_2H_2$, $C_2H_3^+ + HS$, $CH_2CS^+ + H_2$, and $CHCSH^+ + H_2$—are established based on the comparison of experimental AE values and theoretically predicted dissociation energies.

As the dissociation channel c-$C_2H_4S^+ \rightarrow CH_3CS^+ + H$ of least energy likely involves structural alternation during dissociation, substantial kinetic energy is expected to be released on dissociation if reverse activation barriers exist. The

[a)]Author to whom correspondence should be addressed. Fax: (886)3-578-3813. Electronic mail: schiang@nsrrc.org.tw

kinetic energy released after dissociative photoionization is not, however, taken into account in determination of AE from PIMS experiments.[14,15] The previous proposition of formation of an angular structure of HCS^+ from dissociation of c-$C_2H_4S^+$ through a tight and early transition state also needs more experimental and theoretical studies to understand the dissociation mechanisms. Our aim in this work is to investigate the dissociation properties of c-$C_2H_4S^+$ to $CH_3CS^+ + H$ and $HCS^+ + CH_3$ with threshold photoelectron-photoion coincidence (TPEPICO) experiments and quantum-chemical calculations. We measured well-resolved TPEPICO mass spectra of c-C_2H_4S excited at photon energies in a region of 10.6–11.8 eV. From the area and the full width at half maximum (FWHM) of c-$C_2H_4S^+$, CH_3CS^+, and HCS^+ TOF peaks in coincidence mass spectra, we obtained branching ratios and average releases of kinetic energies at various photon energies, and discuss plausible dissociation mechanisms on this basis and from calculations.

II. EXPERIMENTS

Our apparatus is described in detail elsewhere.[16,17] Briefly, we performed coincidence measurements with a molecular-beam/threshold-photoelectron-photoion-coincidence (MB/TPEPICO) system on the Seya-Namioka beamline at the National Synchrotron Radiation Research Center (NSRRC) in Taiwan. Photon energies with resolution of 30 meV and photon flux $>10^9$ photons s^{-1} in a region of 10.6–11.8 eV were selected with Seya-Namioka monochromator (1 m; 1200 grooves mm^{-1}; slit width of 0.15 mm). Absolute photon energies were calibrated within ±0.003 eV on the measurement of Rydberg peaks in the threshold photoelectron spectra (TPES) of Ar and Kr.

c-C_2H_4S and He in a mixture at a total stagnation pressure of 280 Torr and with a seed ratio ~15% were expanded to form a molecular beam. The monochromatic vacuum ultraviolet (VUV) radiation intersected perpendicularly with the beam to ionize cooled c-C_2H_4S molecules in the ionization chamber. The threshold electrons and ions produced were then analyzed with a threshold photoelectron spectrometer and a TOF mass spectrometer, respectively; dual microchannel plates served as detectors in both spectrometers.

A dc field of 1.0 V cm^{-1} in the interaction region was used to extract threshold electrons and a pulsed field of 21 V cm^{-1} with a duration of 30 μs was applied to extract ions on detecting a threshold electron. Signals of detected threshold electrons and ions were fed into a time-to-digital converter (TDC) to record flight durations of ions that were detected within 30 μs of each cycle triggered with a threshold electron. To eliminate a large contribution from uncorrelated ions piling up in the interaction region, a second coincidence spectrum triggered with a signal generated randomly relative to the preceding threshold electron signal was accumulated following each threshold electron-triggered coincidence cycle. Subtraction of the randomly generated coincidence spectrum from the electron-triggered coincidence spectrum yielded a true coincidence spectrum. All data acquisition was controlled with a computer via a computer assisted measurement and control (CAMAC) interface, and output from the TDC converter was transferred to the computer for further processing.

c-C_2H_4S (Aldrich, ~98%) was degassed with several freeze-pump-thaw cycles before use and was kept in an ice bath at 0 °C during experiments. He (>99.999%), Kr (>99.99%), and Ar (>99.99%) were used without further purification.

III. THEORETICAL CALCULATIONS

We calculated the molecular structures and energies of c-C_2H_4S and species pertinent to this work with the Gaussian 3 (G3) method using the GAUSSIAN 2003 program.[18] The equilibrium structure of each species was fully optimized at the MP2(full)/6-31G(d) level and single-point calculations of G3 energy were performed at levels MP4/6-31G(d), QCSID(T)/6-31G(d), MP4/6-31+G(d), MP4/6-31G($2df,p$), and MP2 (full)/G3 large; G3 large is a modified 6-311+G($3df,2p$) basis set. Additional energies include a spin-orbit correction for atomic species, higher-level corrections for atoms and molecules, and a zero-point vibrational energy; the HF/6-31G(d) vibrational frequencies are scaled by 0.8929 and applied for the correction of zero-point vibrational energy. All identified structures were verified to have only real vibrational frequencies at the MP2(full)/6-31G(d) level, except transition structures that have one imaginary vibrational frequency. Transition structures for dissociation channels c-$C_2H_4S^+ \rightarrow CH_3CS^+ + H$ and $HCS^+ + CH_3$ were located in this work; each dissociation path was confirmed with intrinsic reaction coordinate (IRC) calculations.

IV. RESULTS AND DISCUSSION

A. Coincidence TOF spectra in 10.6–11.8 eV

Coincidence mass spectra of c-C_2H_4S having well-resolved TOF peaks were recorded at selected photon energies in a region of 10.6–11.8 eV with 1-ns resolution and corrected for a false coincidence background. Figures 1(a)–1(e) show the corrected coincidence TOF spectra of c-C_2H_4S excited at 9.06, 10.83, 10.88, 10.98, and 11.04 eV; the solid lines indicate the TOF peaks fitted to Gaussian shapes and all spectra are normalized to 7000 total ion counts. Ion signals at $m/z=59$, 60, 61, and 62, corresponding to isomeric structures of $C_2H_3S^+$, c-$C_2H_4S^+$, c-$^{13}C_2H_4S^+$, and c-$C_2H_4{}^{34}S^+$, respectively, were identified according to ion flight durations calculated with an equation $T_o/\text{ns} = 2175.2(m/z)^{1/2} + 231.1$ obtained from coincidence TOF spectra of He, Ar, and Kr excited at photon energies near their ionization thresholds.

In Fig. 1(a), only signals attributed to parent ions c-$C_2H_4S^+$ and their two isotopic variants are observed; no attempt was made to fit the ion signals of those variants at greater photon energies because they were not abundant. The TOF peak of c-$C_2H_4S^+$ fitted to a Gaussian profile has a FWHM of 26 ns; accordingly the transverse temperature of the molecular beam is calculated to be 10 K.[19] This result indicates a small transverse velocity of the skimmed molecular beam along the detection axis and negligible c-$C_2H_4S^+$

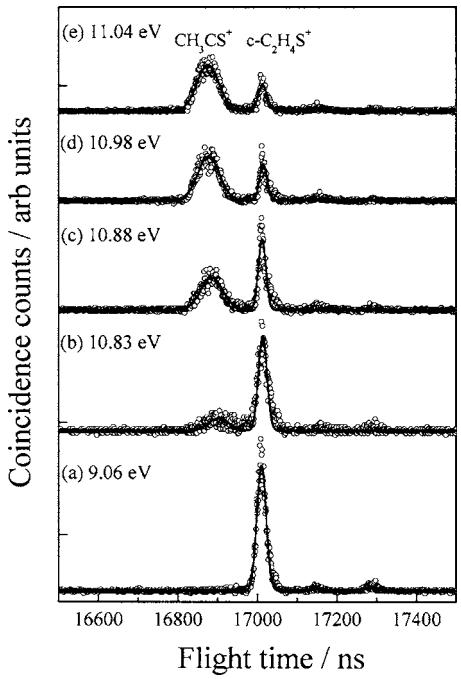

FIG. 1. Coincidence TOF spectrum of c-C_2H_4S excited at photon energies (a) 8.89, (b) 10.83, (c) 10.88, (d) 10.98, and (e) 11.04 eV.

signals resulting from thermal (298 K) background that would broaden a TOF peak. In Figs. 1(b)–1(e), a well-resolved and symmetrically broadened TOF peak of fragment ion $C_2H_3S^+$ is also observed; the broadened TOF peak indicates the substantial release of kinetic energy upon dissociation and its bandwidth and intensity increase with increasing photon energy.

Figures 2(a)–2(e) show corrected coincidence TOF spectra of c-C_2H_4S excited at 11.13, 11.31, 11.50, 11.71, and

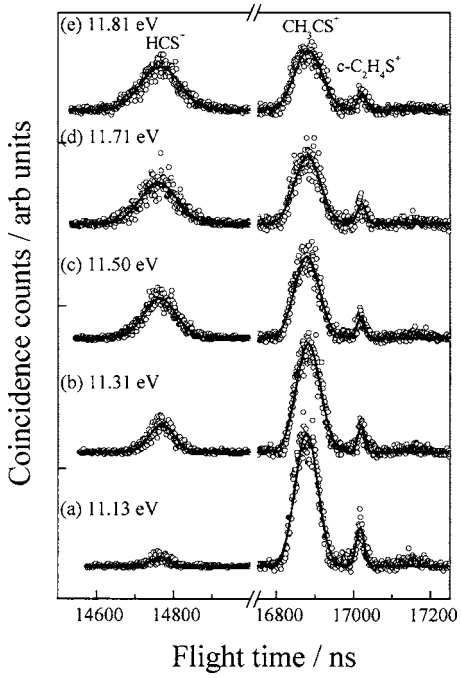

FIG. 2. Coincidence TOF spectrum of c-C_2H_4S excited at photon energies (a) 11.13, (b) 11.31, (c) 11.50, (d) 11.71, and (e) 11.81 eV.

11.81 eV; all spectra are normalized to 7000 total ion counts. In these figures, a broadened TOF peak of fragment ion HCS^+ is observed in addition to those of c-$C_2H_4S^+$ and $C_2H_3S^+$. The broadening also reflects the release of kinetic energy upon dissociation and was fitted well to a Gaussian shape; moreover, its bandwidth and intensity increase with increasing photon energy. Also discernible in the figures, c-$C_2H_4S^+$ signals become less distinct but remain nearly constant at greater photon energies. The constantly small c-$C_2H_4S^+$ signals are attributable to coincidences with hot electrons due to the hot-electron tail function of our threshold electron analyzer, because a continuous background through the Franck-Condon gap region of 10.0–10.7 eV is observed in our TPES and this continuum could extend to a band that is associated with removal of a σ_a electron in the region of 10.9–11.8 eV.[20–22] We observed also a small TOF peak at $m/z=53$, not shown in Figs. 1 and 2, at photon energies smaller than 11.71 eV, but its formation as a result of dissociation of c-$C_2H_4S^+$ is excluded because its TOF peak is narrow, ~20 ns; its source is unclear, but likely an impurity in the sample.

B. Theoretical calculations of dissociation energies and vibrational frequencies

We obtained fully optimized structures [MP2(full)/6-31G(d)] of the five most stable isomers of c-$C_2H_4S^+$–CH_3CHS^+(1), *cis*-CH_2CHSH^+(2a), *trans*-CH_2CHSH^+(2b), c-$C_2H_4S^+$(3), and $CH_2SCH_2^+$(4), three isomers of $C_2H_3S^+$–CH_3CS^+(5), CH_2CSH^+(6), c-$C_2H_3S^+$(7), HCS^+, CH_3, H, and species at local minimum and transition states that occur in isomerization processes of c-$C_2H_4S^+$. Predicted structural parameters for c-$C_2H_4S^+$, $CH_2SCH_2^+$, CH_3CS^+, CH_2CSH^+, and c-$C_2H_3S^+$ agree with previous calculations using varied methods in the literature.[23,24]

Table I lists the calculated G3 energies (E_0/hartree) for species pertinent to this work and Table II lists the predicted ionization energies and dissociation energies (ΔE/eV) calculated from Table I. According to Table II, predicted IE for the formation of CH_3CHS^+(1), *cis*-CH_2CHSH^+(2a), *trans*-CH_2CHSH^+(2b), c-$C_2H_4S^+$(3), and $CH_2SCH_2^+$(4) are 8.85, 8.89, 8.91, 9.07, and 9.37 eV, respectively; CH_3CHS^+ is the most stable structure among the five isomers of c-$C_2H_4S^+$, but *cis*- and *trans*-CH_2CHSH^+ have energies only 0.04 and 0.06 eV greater than that for CH_3CHS^+, respectively. A prediction of 9.07 eV for the formation of c-$C_2H_4S^+$ agrees satisfactorily with literature values IE=9.04±0.01, 9.051±0.003, or 9.051±0.006 eV determined in various experiments;[2,13,15] this result reflects no significant structural alternation from c-C_2H_4S to c-$C_2H_4S^+$ and is associated with removal of a nonbonding electron on the S atom upon ionization.

Predicted dissociation energies for c-C_2H_4S $\rightarrow CH_3CS^+(5)+H$, $CH_2CSH^+(6)+H$, and c-$C_2H_3S^+(7)+H$ are 10.51, 11.61, and 11.74 eV, respectively. CH_3CS^+ has the least energy among three isomers of $C_2H_3S^+$; unstable CH_2CHS^+, unlike CH_2CHSH^+(2a,2b), with one imaginary frequency corresponds to no local minimum. In contrast to

TABLE I. Calculated G3 energies (E_0) for species pertinent to dissociation channels c-$C_2H_4S^+ \rightarrow CH_3CS^+ + H$ and $HCS^+ + CH_3$.

Species	Symmetry	E_0/hartree
c-C_2H_4S	$C_{2v}(^1A_1)$	−476.561 45
CH_3CHS^+(1)	$C_s(^2A')$	−476.236 22
cis-CH_2CHSH^+(2a)	$C_s(^2A'')$	−476.234 75
trans-CH_2CHSH^+(2b)	$C_s(^2A'')$	−476.233 85
c-$C_2H_4S^+$(3)	$C_{2v}(^2B_1)$	−476.228 32
$CH_2SCH_2^+$(4)	$C_{2v}(^2A_2)$	−476.217 04
CH_3CS^+(5)	$C_{3v}(^1A_1)$	−475.674 11
CH_2CSH^+(6)	$C_s(^1A')$	−475.633 77
c-$C_2H_3S^+$(7)	$C_s(^1A')$	−475.628 84
HCS^+	$C_{\infty v}(^1\Sigma)$	−436.361 96
CH_3	$D_{3h}(^2A''_2)$	−39.793 30
H	(^2S)	−0.501 00
TS1	$C_1(^2A)$	−476.156 71
TS1-2	$C_1(^2A)$	−476.187 02
TS2	$C_1(^2A)$	−476.180 50
TS3	$C_1(^2A)$	−476.159 87
TS4	$C_s(^2A')$	−476.164 09
LM1-1	$C_1(^2A)$	−476.187 43
LM1-2	$C_1(^2A)$	−476.187 68
LM3	$C_s(^2A')$	−476.199 97

dissociation c-$C_2H_4O^+ \rightarrow c$-$C_2H_3O^+ + H$ reported previously,[25] the formation of c-$C_2H_3S^+$ is excluded as its predicted dissociation energy of 11.74 eV is much greater than the experimental AE value of 10.71±0.01 eV determined in PIMS experiments;[2,13] CH_3CS^+ is the most likely structure on energetic grounds despite a small difference of 0.2 eV between predicted and experimental values.

A predicted dissociation energy of 11.05 eV for c-$C_2H_4S \rightarrow HCS^+ + CH_3$ is near previously reported AE values of 11.13±0.04 and 11.13±0.01 eV for the formation of HCS^+.[2,13] This small discrepancy supports an observation of a small release of kinetic energy near the dissociation threshold reported from a previous PEPICO investigation and in this work, which are discussed later. Especially noteworthy is our predicted structure of HCS^+ at the threshold that is linear, not angular as reported previously;[1] a previous proposition of a tight and early transition state for this dissociation channel to form a bent HCS^+ is thus excluded.

TABLE II. Predicted ionization energies and relative energies (ΔE) for species pertinent to this work.

Species	ΔE/eV
c-$C_2H_4S \rightarrow CH_3CHS^+$(1)	8.85
$\rightarrow$*cis*-CH_2CHSH^+(2a)	8.89
$\rightarrow$*trans*-CH_2CHSH^+(2b)	8.91
$\rightarrow c$-$C_2H_4S^+$(3)	9.07
$\rightarrow CH_2SCH_2^+$(4)	9.37
$\rightarrow CH_3CS^+(5) + H$	10.51
$\rightarrow CH_2CSH^+(6) + H$	11.61
$\rightarrow c$-$C_2H_3S^+(7) + H$	11.74
$\rightarrow HCS^+ + CH_3$	11.05
$\rightarrow$TS1	11.01
$\rightarrow$TS1-2	10.19
$\rightarrow$TS2	10.37
$\rightarrow$TS3	10.93
$\rightarrow$TS4	10.81
$\rightarrow$LM1-1	10.18
$\rightarrow$LM1-2	10.17
$\rightarrow$LM3	9.84

TABLE III. Vibrational wave numbers of ground-state CH_3CS^+ and HCS^+ calculated at the HF level and scaled by 0.8929.

Ion	Modes	Vibrational wave numbers/cm^{-1}
CH_3CS^+	$\upsilon_1(e)$	2937
	$\upsilon_2(a_1)$	2852
	$\upsilon_3(a_1)$	1585
	$\upsilon_4(e)$	1381
	$\upsilon_5(a_1)$	1365
	$\upsilon_6(e)$	991
	$\upsilon_7(a_1)$	715
	$\upsilon_8(e)$	336
HCS^+	$\upsilon_1(\sigma)$	3122
	$\upsilon_2(\pi)$	788
	$\upsilon_3(\sigma)$	1421

Vibrational wave numbers of CH_3CHS^+ for eight normal modes and of HCS^+ for four normal modes in their ground states calculated at the HF/6-31G(d) level and scaled by 0.8929 are listed in Table III and used for subsequent quasiequilibrium theory (QET) calculations. Scaled vibrational wave numbers 3122 and 788 cm^{-1} for HCS^+ are consistent with the experimental values of 3141 and 766 cm^{-1}.[26]

C. Branching ratios and average releases of kinetic energy

Figure 3 shows the branching ratios of c-$C_2H_4S^+$ and fragment ions CH_3CS^+ and HCS^+ in the region of 10.6–11.8 eV obtained from the area ratios of TOF peaks in coincidence spectra. Fragment ion CH_3CS^+ appears at threshold ~10.76 eV and then increases to a crossing point with c-$C_2H_4S^+$ at 10.87 eV before reaching a maximum at ~11.18 eV, after which it diminishes toward greater photon energies because of the formation of HCS^+. Fragment ion HCS^+ appears at an onset ~11.13 eV that lies between the onset at ~10.7 eV and the maximum at 11.37 eV of the first excited electronic state of c-$C_2H_4S^+$; formation of HCS^+ is thus likely due to a new dissociation channel opening as the

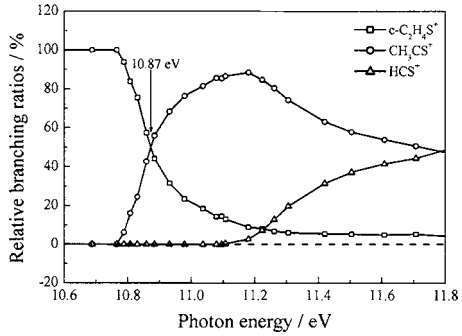

FIG. 3. Branching ratios of c-$C_2H_4S^+$, CH_3CS^+, and HCS^+ in a region 10.6–11.8 eV; fractional abundances of these three ions were obtained from their total signals.

TABLE IV. Calculated average release of kinetic energies from the full width at half maximum (FWHM) at selected photon energies for dissociation channels c-$C_2H_4S^+ \rightarrow CH_3CS^+ + H$ and $HCS^+ + CH_3$.

	CH_3CS^+		HCS^+	
PE/eV	FWHM/ns	⟨KE⟩/eV	FWHM/ns	⟨KE⟩/eV
10.83	62.4	0.434	-	-
10.86	62.4	0.434	-	-
10.88	62.4	0.434	-	-
10.93	63.9	0.459	-	-
10.98	64.9	0.475	-	-
11.04	65.1	0.479	-	-
11.08	66.3	0.500	-	-
11.10	67.5	0.520	-	-
11.11	68.4	0.537	-	-
11.13	69.5	0.556	59.7	0.037
11.18	69.0	0.548	61.0	0.039
11.22	72.2	0.607	62.0	0.040
11.26	73.5	0.631	73.9	0.059
11.31	74.1	0.642	76.1	0.063
11.42	75.5	0.670	91.8	0.093
11.50	76.3	0.686	100.3	0.112
11.61	78.3	0.727	107.9	0.130
11.71	80.5	0.774	116.6	0.152
11.81	85.2	0.876	122.8	0.170

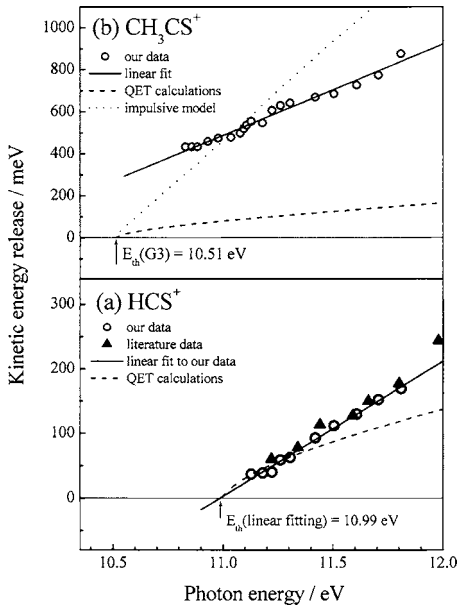

FIG. 4. Average kinetic energy released into dissociation channels c-$C_2H_4S^+ \rightarrow$ (a)$HCS^+ + CH_3$ and (b) $CH_3CS^+ + H$ with excitation at photon energies in a region 10.6–11.8 eV. Data, a line fitted to data, QET calculations, and a calculation according to an impulsive model are marked as circles, solid line, dashed line and dotted line, respectively; literature data in (a) are marked as solid triangles for comparison.

internal energy of the parent ion c-$C_2H_4S^+$ increases. The small signals of c-$C_2H_4S^+$ remain constant at greater photon energies likely because of coincidences with hot electrons, as mentioned above.

The broadened TOF peak for each fragment ion is well fitted with a Gaussian shape. In general, for a distribution of this type, the average release of kinetic energy (KE) is related to the FWHM of the TOF peak and calculated from that FWHM according to the Maxwellian equation[19,27]

$$\langle \mathrm{KE} \rangle = \frac{3}{15 \ln 2} \varepsilon^2 (\mathrm{FWHM})^2 \frac{M_p}{M_f (M_p - M_f)} - \frac{3}{2} RT \frac{M_f}{(M_p - M_f)}, \quad (1)$$

in which ⟨KE⟩ is the average release of kinetic energy, $\varepsilon = 21$ V cm^{-1} is the strength of the pulsed electric field for ion extraction, FWHM is obtained from the fitted TOF peak of a fragment ion, M_p and M_f are masses of parent and fragment ions, and $T = 10$ K is the transverse temperature of the molecular beam. Obtained FWHM and calculated average release of kinetic energy for both dissociation channels at selected photon energies in the region of 10.6–11.8 eV are listed in Table IV. As a pulsed delay extraction might narrow a TOF peak that is broadened because kinetic energy is released, we calculated this effect on our derived ⟨KE⟩ based on a delay of ~231 ns between a threshold photoelectron detection and a pulsed extraction field from the equation $T_o/\mathrm{ns} = 2175.2(m/z)^{1/2} + 231.1$. Within the delay, fragment ions CH_3CS^+ move ~0.04–0.06 mm away from the interaction region in the weak field 1 V cm^{-1} according to average releases ~0.4–0.88 eV of kinetic energy obtained in this work for channel $CH_3CS^+ + H$, and fragment ions HCS^+ move ~0.08–0.1 mm with average releases ~0.04–0.17 eV of kinetic energy for channel $HCS^+ + CH_3$. Because of the small displacements of both fragment ions CH_3CS^+ and HCS^+, the effect on narrowing a TOF peak before a pulsed high-voltage applied is expected to be negligible.

In Figs. 4(a) and 4(b), calculated average releases of kinetic energy for channels $HCS^+ + CH_3$ and $CH_3CS^+ + H$ are depicted as circles, respectively. For channel $HCS^+ + CH_3$, a solid line for a linear fit to our data, a dashed curve for QET calculations, and solid triangles representing literature data of Butler and Baer[1] are also depicted in Fig. 4(a) for comparison. The QET calculations were performed according to an equation formulated by Klots[28–30]

$$h\nu - E_0 = \frac{(r+1)}{2} \langle \mathrm{KE} \rangle + \sum_i \frac{h\nu_i}{\exp(h\nu_i / \langle \mathrm{KE} \rangle) - 1}, \quad (2)$$

in which $h\nu$ is the photon energy, $E_0 = 10.99 \pm 0.04$ eV derived from linear extrapolation of our experimental data, is the dissociation threshold for the formation of HCS^+ and CH_3, r is the number of rotational degrees of freedom of products (two for HCS^+ and three for CH_3), and ν_i are the vibrational wave numbers of CH_3 and HCS^+; vibrational wave numbers 3004.4, 606.5, 3160.8, and 1396 cm^{-1} for CH_3 are taken from the literature[31] and those of HCS^+ are listed in Table III.

As seen in Fig. 4(a), our data agree satisfactorily with literature values; our linearly extrapolated threshold at 10.99 ± 0.04 eV also agrees with a predicted dissociation energy of 11.05 eV for formation of linear HCS^+ and CH_3 from c-C_2H_4S. Although significant differences are observed at greater photon energies, QET results seem to fit well the experimental data near the dissociation threshold; accordingly, the average release of kinetic energy is 0.037 eV at the

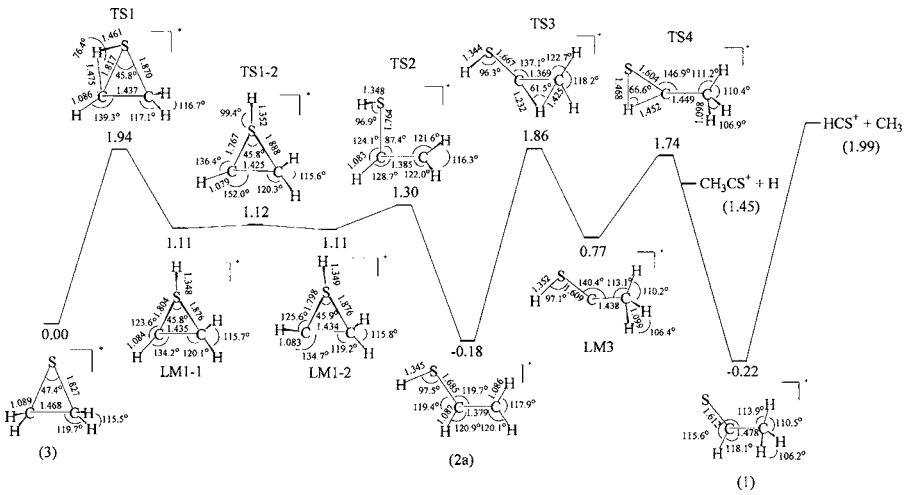

FIG. 5. Theoretical predictions of relative energies in eV for isomerization of c-$C_2H_4S^+$ into CH_3CHS^+ before dissociation into channels CH_3CS^++H and HCS^++CH_3; bond lengths in angstroms and interbond angles in degrees are indicated for molecular structures optimized at the MP2 (full)/6-31G(d) level.

AE value of 11.13 eV for HCS^+ determined in previous PIMS studies of c-C_2H_4S. Because formation of HCS^+ and CH_3 likely involves H migration before dissociation occurs, the agreement of an extrapolated threshold with a G3 prediction and small releases of kinetic energy near the dissociation threshold imply that the energy for isomerization of c-$C_2H_4S^+$ into the dissociation precursor lies below or near the dissociation threshold.

For channel CH_3CS^++H, a linear solid line fitted to data, a dashed curve for QET calculations, and a dotted line for calculations based on a pure impulsive model[32,33] are depicted in Fig. 4(b) for comparison. In QET calculations, a predicted dissociation energy of 10.51 eV for c-$C_2H_4S^+ \rightarrow CH_3CS^+$+H was taken as the dissociation threshold because, to our knowledge, no experimental dissociation threshold is available, except the experimental AE of 10.71 ± 0.01 eV for CH_3CS^+ determined in previous PIMS studies. Calculations based on a pure impulsive model were performed with a simple equation

$$\langle \mathrm{KE} \rangle = (\mu_b/\mu_f) E_{\mathrm{avl}}, \tag{3}$$

in which μ_b is the reduced mass of the two atoms (C and H) between which a bond is broken, μ_f is the reduced mass of the two products (CH_3CS^+ and H), and $E_{\mathrm{avl}}=h\nu-E_0$ is the difference between photon energies and dissociation threshold (E_0); $E_0=10.51$ eV is taken from a G3 prediction, as explained above.

As seen in Fig. 4(b), unlike channel HCS^++CH_3, measured releases of kinetic energy for channel CH_3CS^++H are substantial, but results of QET calculations lie far below experimental values; moreover, a linearly extrapolated threshold at 9.87 eV for this channel is much smaller than a G3 prediction of 10.51 eV and the experimental AE of 10.71 ± 0.01 eV.[2,13] A nonstatistical distribution of measured substantial kinetic energies and the discrepancies at the dissociation threshold indicate that dissociation occurs through a dissociative excited state or involves substantial exit barriers. The presence of substantial exit barriers for formation of CH_3CS^+ is likely due to H migration and structural alternations during dissociation. On the other hand, the existence of a dissociative excited state in a region of 10.51–10.71 eV is excluded because there is no electronic state but a Franck-Condon gap in a region of ~10.0–10.7 eV according to a previously reported photoelectron spectrum and our threshold photoelectron spectrum.[20–22] Moreover, an impulsive model is generally applied to the dissociation that proceeds rapidly from a repulsive dissociative potential-energy surface, but our calculations based on an impulsive model do not fit well the experimental data.

D. Dissociation mechanisms

Figure 5 shows relative energies of a feasible dissociation mechanism for channels c-$C_2H_4S^+ \rightarrow CH_3CS^+$+H and HCS^++CH_3 predicted with the G3 method; structural parameters for the stationary states are labeled in the figure. In Fig. 5, c-$C_2H_4S^+$ first undergoes H migration to form a local minimum c-$CHCH_2SH^+$ (LM1-1) via a transition state TS1; a G3 barrier for this process is 1.94 eV. Next, the H atom of the CH group of c-$CHCH_2SH^+$ (LM1-1) rotates with nearly no barrier to form its *trans*-isomer c-$CHCH_2SH^+$ (LM1-2), which subsequently proceeds through ring opening and C-S bond breaking to form *cis*-CH_2CHSH^+ (2a) via TS2 with a G3 barrier at 1.30 eV. In further formation of CH_3CSH^+ (LM3) and the most stable isomer CH_3CHS^+ (1), the intermediate *cis*-CH_2CHSH^+ (2a) proceeds through H migrations from the CH group to the CH_2 group and from the SH group to the central C atom via TS3 and TS4 with predicted barriers at 1.86 and 1.74 eV, respectively. As dissociation of CH_3CHS^+ (1) to form CH_3CS^++H involves only direct cleavage of the C-H bond, one would expect to find a completely statistical distribution of energy, which is not observed in our experiments. In contrast, if dissociation of CH_3CSH^+ (LM3) to form CH_3CS^++H takes place via TS4, substantial kinetic energies are expected to be released during dissociation, compatible with experimental observations. The predicted barrier of TS4 at 1.74 eV agrees with a difference of 1.66 eV between the experimental AE of 10.71 eV and IE of 9.05 eV determined in previous PIMS studies.[13,15] Although a predicted barrier of 1.94 eV for isomerization of c-$C_2H_4S^+$ to the dissociation precursor CH_3CSH^+ (LM3) is slightly greater than the predicted barrier of TS4 at 1.74 eV, but still within an uncertainty of theoretical calculations for transition states. We sought to break the C-S bond directly to form a ring-opened structure $CH_2CH_2S^+$, which can proceed

through H migrations from one CH_2 group to the other CH_2 group to form CH_3CHS^+, but located no transition state for this process. Although BelBruno predicted a smaller activation barrier of 1.87 eV for isomerization of c-$C_2H_4S^+$ into $CH_2SCH_2^+$,[23] this dissociation mechanism is unexpected because of the weakness of the C-S bond relative to the C-C bond.

For channel $HCS^+ + CH_3$, Fig. 5 shows that dissociation of CH_3CHS^+ (1) to form $HCS^+ + CH_3$ proceeds through direct cleavage of the C-C bond without an exit barrier and would result in a statistical energy distribution in the dissociation; a predicted G3 barrier of 1.94 eV for isomerization of c-$C_2H_4S^+$ to CH_3CHS^+ (1) is nearly the same as a predicted dissociation energy of 1.99 eV. The results of a predicted negligible barrier and a statistical distribution of energy in the dissociation agree satisfactorily with experimental observations.

V. CONCLUSION

Dissociation of energy-selected c-$C_2H_4S^+$ into channels $CH_3CS^+ + H$ and $HCS^+ + CH_3$ was investigated in a region of 10.6–11.8 eV with a TPEPICO technique in pulsed mode and quantum-chemical calculations. Branching ratios for c-$C_2H_4S^+$, CH_3CS^+, and HCS^+ and average releases of kinetic energy for CH_3CS^+ and HCS^+ were derived from well-resolved TOF peaks in coincidence spectra. Small releases of kinetic energy for formation of HCS^+ agree with QET calculations near the appearance threshold, but substantial releases of kinetic energy for formation of CH_3CS^+ differ significantly from statistical calculations. A detailed energy profile for dissociation mechanisms of c-$C_2H_4S^+$ to form $CH_3CS^+ + H$ and $HCS^+ + CH_3$ is reported based on the calculations with the Gaussian 3 method. A large kinetic energy released on the formation of $CH_3CS^+ + H$ is probably due to a reverse activation barrier required for dissociation of CH_3CSH^+(LM3) through a transition state; in contrast, the statistical energy distribution for formation of $HCS^+ + CH_3$ is due to dissociation of the most stable isomer CH_3CHS^+ without an exit barrier.

ACKNOWLEDGMENTS

The National Synchrotron Radiation Research Center and the National Science Council of Taiwan (Contract No. NSC92-2113-M-213-001) provided financial support, and the National Center for High-Performance Computing provided computing time for theoretical calculations.

[1] J. J. Butler and T. Baer, J. Am. Chem. Soc. **104**, 5016 (1982).
[2] J. J. Bulter and T. Baer, Org. Mass Spectrom. **18**, 248 (1983).
[3] F. Qi, O. Sorkhabi, and A. G. Suits, J. Chem. Phys. **112**, 10707 (2000).
[4] J. W. Gardiner, *Combustion Chemistry* (Springer, New York, 1984).
[5] M. B. Robin, *Higher Excited States of Polyatomic Molecules* (Academic, New York, 1985).
[6] A. S. Bodke, D. A. Olschki, L. D. Schmidt, and E. Ranzi, Science **285**, 712 (1999).
[7] M. C. Pirrung, Acc. Chem. Res. **32**, 711 (1999).
[8] T. R. Younkin, E. F. Connor, J. I. Henderson, S. K. Friedrich, R. H. Grubbs, and D. A. Bansleben, Science **287**, 460 (2000).
[9] H. L. Kim, S. Satyapal, P. Brewer, and R. Bersohn, J. Chem. Phys. **91**, 1047 (1989).
[10] P. Felder, E. A. J. Wannenmacher, I. Wiedmer, and J. R. Huber, J. Phys. Chem. **96**, 4470 (1992).
[11] F. Qi, O. Sorkhabi, A. G. Suits, S.-H. Chien, and W.-K. Li, J. Am. Chem. Soc. **123**, 148 (2001).
[12] E. M. Lown, K. S. Sidhu, A. W. Jackson, A. Jodhan, M. Green, and O. P. Strausz, J. Phys. Chem. **85**, 1089 (1981).
[13] S.-Y. Chiang and Y.-S. Fang, J. Electron Spectrosc. Relat. Phenom. **144**, 223 (2005).
[14] B. P. Tsai, T. Baer, A. S. Werner, and S. F. Lin, J. Phys. Chem. **79**, 570 (1975).
[15] H. Shiromaru, Y. Achiba, and Y. T. Lee, J. Phys. Chem. **91**, 17 (1987).
[16] S.-Y. Chiang and C.-I Ma, J. Phys. Chem. A **104**, 1991 (2000).
[17] S.-Y. Chiang, Y.-C. Lee, and Y.-P. Lee, J. Phys. Chem. A **105**, 1226 (2001).
[18] M. J. Frisch, G. W. Trucks, H. B. Schlegel, *et al.*, Gaussian, Inc., Pittsburgh, PA, 2003.
[19] R. Stockbauer, Int. J. Mass Spectrom. Ion Phys. **25**, 89 (1977).
[20] D. H. Aue, H. M. Webb, W. R. Davidson, *et al.*, J. Am. Chem. Soc. **102**, 5151 (1980).
[21] D. C. Frost, F. G. Herring, A. Katrib, and C. A. McDowell, Chem. Phys. Lett. **20**, 401 (1973).
[22] A. Schweig and W. Thiel, Chem. Phys. Lett. **21**, 541 (1973).
[23] J. J. BelBruno, Chem. Phys. Lett. **254**, 321 (1996).
[24] S.-W. Chiu, K.-C. Lau, and W.-K. Li, J. Phys. Chem. A **104**, 3028 (2000).
[25] F. Liu, F. Qi, H. Gao, L. Sheng, Y. Zhang, S. Yu, K.-C. Lau, and W.-K. Li, J. Phys. Chem. A **103**, 4155 (1999).
[26] P. J. Linstrom and W. G. Mallard, *NIST Chemistry Webbook, NIST Standard Reference Database No. 69*, 2005 Release (http://webbook.nist.gov).
[27] T. Baer, G. D. Whillett, D. Smith, and J. S. Phillips, J. Chem. Phys. **70**, 4076 (1979).
[28] C. E. Klots, J. Chem. Phys. **58**, 5364 (1973).
[29] C. E. Klots, Adv. Mass Spectrom. **6**, 969 (1974).
[30] C. E. Klots, J. Chem. Phys. **64**, 4269 (1976).
[31] M. E. Jacox, J. Phys. Chem. Ref. Data **32**, 157 (2003).
[32] G. E. Busch and K. R. Wilson, J. Chem. Phys. **56**, 3626 (1972).
[33] K. E. Holdy, L. C. Klotz, and K. R. Wilson, J. Chem. Phys. **52**, 4588 (1970).